β-Lactoglobulin as a nanotransporter for glabridin: exploring the binding properties and bioactivity influences

by Wei, Y., Vriesekoop, F., Yuan, Q. and Liang, H.

DOI: 10.1021/acsomega.8b01576

Wei, Y., Vriesekoop, F., Yuan, Q. and Liang, H. 2018. β-Lactoglobulin as a nanotransporter for glabridin: xxploring the binding properties and bioactivity influences. *ACS Omega*, 3(9), pp.12246 – 12252.

ACS OMEGA

Article

Cite This: ACS Omega 2018, 3, 12246−12252

http://pubs.acs.org/journal/acsodf

β-Lactoglobulin as a Nanotransporter for Glabridin: Exploring the Binding Properties and Bioactivity Influences

Yongqin Wei,[†] Frank Vriesekoop,[‡] Qipeng Yuan,[†] and Hao Liang*[,†]

[†]State Key Laboratory of Chemical Resource Engineering, Beijing University of Chemical Technology, Beijing100029, P. R. China

[‡]Department of Food Science, Harper Adams University, Newport TF10 8NB, Shropshire, England

Supporting Information

ABSTRACT: Based on the fact that β-lactoglobulin (β-lg) can solubilize readily in water and bind many small hydrophobic molecules, a novel nanocomplexed glabridin with β-lg was developed by an antisolvent precipitation method. After binding to β-lg, the solubility of glabridin in aqueous solution was enhanced 21 times. Fluorescence spectroscopy of β-lg revealed that the interaction of glabridin with β-lg made the environment of Trp and Tyr residues on β-lg more hydrophilic. The morphology and crystal form of the nanocomplexed glabridin with β-lg was characterized and the changes in β-lg conformation was also been investigated. In combination with molecular docking modeling, the results revealed that glabridin was bound to β-lg by hydrophobic forces and hydrogen-bond interactions. Furthermore, the nanocomplexed glabridin with β-lg had a better 2,2-diphenyl-1-picrylhydrazyl radical-scavenging capacity and 2,2′-azino-bis-3-ethylbenzthiazoline-6-sulfonic acid radical-scavenging capacity compared to free glabridin at the same concentration during in vitro tests. Thus, nanocomplexing with β-lg, by virtue of its ability to enhance the solubility of glabridin in aqueous systems, provides a suitable opportunity as a nanocarrier molecule.

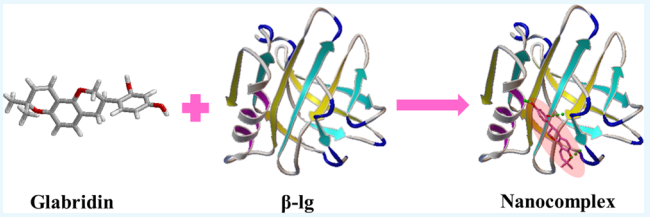

INTRODUCTION

Glabridin (Figure 1a) is an isoflavonoid found in the roots of *Glycyrrhiza glabra* L. (Favaceae), commonly known as licorice.[1] A wide range of pharmacological properties of glabridin have been reported, including antioxidation,[2,3] inhibiting melanogenesis,[4,5] anti-inflammation,[6] estrogen-like activity, antiproliferative activity in regards to cancer cells,[7,8] enhancing memory,[9] etc. Glabridin has significant applications in food, dietary supplements, and cosmetic markets. However, the practical application of glabridin is extremely limited owing to its poor aqueous solubility and, thus, poor bioavailability, as well as its unpredictable stability.[10]

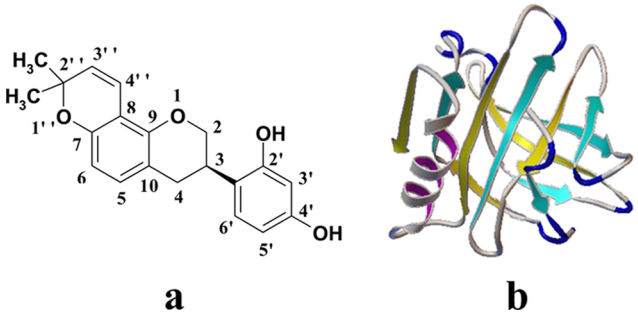

Figure 1. (a) Chemical structure of glabridin and (b) three-dimensional structure of β-lactoglobulin.

β-Lactoglobulin (β-lg, Figure 1b) is a bovine whey protein that has been one of the most extensively investigated proteins due to its abundant presence. It is consists of a polypeptide chain of 162 amino acid residues and exhibits an average molecular weight of 18 400 Da, with a isoelectric point (pI) about pH 5.1−5.2.[11] This small globular protein belongs to the lipocalin family[12] and has a three-dimensional structure that constitutes a hydrophobic pocket consisting of eight strands of antiparallel β-sheet twisted into a cone-shaped barrel.[13] The special hydrophobic pocket structure provides a high-affinity environment to small hydrophobic ligands such as lipid,[14,15] fatty acid,[16−18] aromatic compounds,[19,20] and lipophilic vitamins.[21,22] Besides, there are also some other reported binding sites on β-lg, such as the hydrophobic groove between β-helix and β-barrel outer surface, the outer surface site near the bottom of calyx in close proximity to Trp19 and Arg124,[23,24] and near the cleft of dimerization interface.[25] As a naturally occurring polymer, β-lg exhibits a low toxicity and better biocompatibility and biodegradability compared to synthetic polymers.[26] Hence, β-lg is an attractive candidate as a natural nanocarrier for delivering important hydrophobic nutrients.

The purpose of the present study was to characterize the interactions of glabridin with β-lg to make a contribution to deeper understanding of the molecular recognition properties of this lipocalin. The stability and structural behavior of gliabridin complexing with β-lg were investigated under

Received: July 9, 2018
Accepted: September 13, 2018
Published: September 28, 2018

DOI: 10.1021/acsomega.8b01576
ACS Omega 2018, 3, 12246−12252

different conditions such as pH, ionic strength, and temperature and examined first by fluorescence spectroscopy. Then, to obtain an in-depth understanding of binding mechanism at the molecular level, the interactions of glabridin with β-lg were investigated by scanning electron microscopy (SEM), X-ray diffractometry (XRD), Fourier transform infrared spectroscopy (FT-IR), circular dichroism (CD), and molecular docking. The solubility of the nanocomplexed glabridin with β-lg in pure water was examined. In addition, the 2,2-diphenyl-1-picrylhydrazyl (DPPH) radical-scavenging capacity and 2,2′-azino-bis-3-ethylbenzthiazoline-6-sulfonic acid (ABTS) radical-scavenging capacity of the formed nanocomplexed glabridin with β-lg were tested and compared to free glabridin.

MATERIALS AND METHODS

Materials. Glabridin (95% purity) was purchased from Hunan Jiamu Biotechnology (Hunan, China). β-lg (90% in purity) was obtained from Energy Chemical (Shanghai, China). 2,2-Diphenyl-1-picrylhydrazyl radical (DPPH, 96% in purity) and 2,2′-azino-bis-3-ethylbenzthiazoline-6-sulfonic acid (ABTS, 98% in purity) were obtained from Sigma Chemical Company (Shanghai, China). All other reagents were of analytical grade and used without further purification.

High-Performance Liquid Chromatography Analysis. Reverse-phase high-performance liquid chromatography (RP-HPLC, CBM-102 communications bus module with a SPD-10A UV−vis detector) was used to quantify glabridin. Separation was carried on a Diamonsil C18 analytical column (4.6 mm × 250 mm, 5 μm) with acetonitrile−2% acetic acid (50:50, v/v) as the mobile phase at a flow rate of 1.0 mL/min. The ultraviolet (UV) detection wavelength was 282 nm.

Preparation of Amorphous Nanocomplexed Glabridin with β-lg. A simple antisolvent precipitation method was adopted to prepare the amorphous nanocomplexed glabridin with β-lg. Briefly, 300 mg of β-lg was completely dissolved in 100 mL phosphate-buffered saline buffer (pH 7.4) as the antisolvent phase and 40 mg of glabridin was completely dissolved in 10 mL ethanol as the solvent phase. Initially, both the solvent and antisolvent phases were cooled to 4 °C. After that, the solvent phase was added to the antisolvent phase while continuously stirring at 800 rpm for 60 min at room temperature. The resulting suspension was exposed to ultrasonic waves for 15 min. Finally, the sample was evaporated under reduced pressure in a rotary evaporator at 40 °C to remove the solvent.

Fluorescence Spectroscopy. The binding and alignment of glabridin with β-lg was investigated by fluorescence spectrophotometry, according to the method of Liang et al.[19] Protein fluorescence was measured at a constant β-lg concentration (10 μM) in the presence of glabridin at various concentrations (0−40 μM) following acclimatization at 37 °C in a water bath for 20 min. The excitation and emission slit widths were 5 nm. Emission spectra were recorded over a range from 300 to 500 nm at an excitation wavelength of 280 nm by employing a Shimadzu RF 5000 spectrofluorimeter. Buffer and ligand backgrounds were subtracted from the raw spectra. Moreover, variables including pH (3.0, 5.2, 7.4, and 10.0), temperature (25, 40, 50, and 60 °C), and ionic strength (0, 100, 200, 300, and 400 mM), which effected the binding fluorescence spectra of glabridin and β-lg, were also studied.

Solubility Study. Excess amount of glabridin (10 mg) or nanocomplexed glabridin with β-lg (20 mg) were added into 1 mL of water. The suspensions were then stirred at 37 °C for 72 h. After that, the samples were filtered through a 0.22 μm membrane filter to remove excess insoluble substances and the filtrate was diluted with ethanol. The amount of glabridin dissolved was calculated using RP-HPLC.

Scanning Electron Microscopy (SEM). The surface morphologies of glabridin, β-lg, the physical mixture, and the nanocomplexed glabridin with β-lg were recorded using a HITACHI S-4700 scanning electron microscope (Japan). All the samples were fixed on a brass stub using double-sided adhesive tape and then sputter coated with a thin layer of gold for electric conductivity before analysis.

X-ray Diffractometry (XRD). The X-ray diffraction patterns of glabridin, β-lg, the physical mixture, and the nanocomplexed glabridin with β-lg were recorded on an X-ray diffractometer (D8 ADVANCE, Germany, Bruker) equipped with a copper target X-ray tube. The voltage and current applied were set at 40 kV and 40 mA, respectively. All the samples were measured over a diffraction angle of 2θ ranging from 5 to 40° at a scan rate of 10°/min and a step size of 0.2°.

Fourier Transform Infrared Spectroscopy (FT-IR). FT-IR spectra of glabridin, β-lg, the physical mixture, and the nanocomplexed glabridin with β-lg were measured on a FT-IR spectrometer (Nicolet 6700) equipped with a DLaTGS detector. The spectral measurements were carried out in the range of 4000 and 400 cm^{-1} with the KBr disk method.

Circular Dichroism (CD). Circular Dichroism (CD) spectra in the wavelength range 200−325 nm were recorded on a Jasco J-810 spectropolarimeter and the measurements were carried out using a 1 mm path length quartz cell. An average of three scans at a speed of 50 nm/min with a bandwidth of 1 nm and a response time of 0.125 s were recorded. The concentration of β-lg used was 0.2 mg/mL, and buffer background was subtracted from the raw spectra.

Molecular Docking Study. In this study, a docking study was carried out to visualize the binding configuration of glabridin to β-lg using the AutoDock empirical free energy scoring function and the Lamarckian genetic algorithm with local search. The docked conformations of nanocomplexes were generated using the AutoDock 4.2.6 program package. The structure of β-lg was taken from RSCB protein data bank (http://www.rcsb.org/pdb). The AutoDock Tools 1.5.6 graphical interface was used to remove water molecules from the structure of β-lg and to add polar hydrogen atoms and partial charges using Gasteiger charges. Then, the entire β-lg molecule was considered to be the search space, and the center of the grid box was determined with a grid spacing of 0.375 Å to allow the ligand to rotate freely.

DPPH Radical-Scavenging Capacity. DPPH free radical-scavenging capacities of glabridin and nanocomplexed glabridin with β-lg were evaluated according to the method of Shimada et al.[27] Briefly, 2 mL aqueous solution of the test samples (glabridin or nanocomplex) of various concentrations (0.5, 1, 4, 6, 10, and 13 μg/mL) were added to 2 mL ethanol solution of DPPH radical (2×10^{-4} mol/L) and then the mixtures were incubated in the dark for 30 min after vortexing. The decrease in the absorbance at 517 nm was measured using a UV-2450 spectrophotometer (Shimadzua, Japan) against an ethanol blank. The scavenging capacity of the samples (SA %) on DPPH were calculated according to the equation

$$\mathrm{SA}\ (\%) = \frac{A_0 - (A_i - A_j)}{A_0} \times 100\%$$

DOI: 10.1021/acsomega.8b01576
ACS Omega 2018, 3, 12246−12252

where A_i is the absorbance of the mixture of 2 mL DPPH solution and 2 mL test sample solution, A_j is the absorbance of the mixture of 2 mL test sample solution and 2 mL ethanol, and A_0 is the absorbance of the mixture of 2 mL DPPH solution and 2 mL ethanol.

ABTS Radical-Scavenging Capacity. The ABTS radical-scavenging activity was measured as described by Li et al.,[28] with some modifications. The ABTS solution was produced by mixing 0.2 mL ABTS diammonium salt (7.4 mM) with 0.2 mL ammonium persulfate (2.6 mM). The mixture was kept in the dark at room temperature for 12 h to allow completion of radical generation and then diluted with ethanol until its absorbance at 734 nm was near 0.74 ± 0.03. To determine the scavenging activity, 0.6 mL aliquot of ABTS reagent was mixed with 150 μL of the sample ethanolic solutions (2−20 μg/mL). After incubation for 6 min, the absorbance at 734 nm was measured on a spectrophotometer. The percentage inhibition of the samples was calculated as

$$\text{inhibition } \% = \frac{A_0 - A}{A_0} \times 100\%$$

where A_0 is the absorbance at 734 nm without the test sample, whereas A is the absorbance at 734 nm with the test sample.

Statistical Analysis. All the analytical experiments were carried out in three replicates and the results were presented as a mean ± standard deviation. One-way analysis of variance was employed to identify significant differences ($p < 0.05$) between the data sets using the software Origin 8.5.

RESULTS AND DISCUSSION

Fluorescence Spectra of β-lg with Glabridin Bound. Proteins possess endogenous fluorescence due to the existence of chromophoric groups on a variety of amino acids such as phenylalanine, tyrosine, and tryptophan. The maximum emission wavelength of various amino residues on proteins are related to the hydrophobicity of their own microenvironment. Furthermore, the fluorescence intensity of any fluorescent substance is reduced in the presence of a fluorescent quencher such as glabridin. Therefore, the migration of the wavelength can be used as a basis for judging whether the conformation of the protein changes.[29] Figure 2 shows the fluorescence emission spectra of β-lg in the presence of different concentrations of glabridin. The intensity of the fluorescence emission of β-lg at around 325 nm gradually decreased and upshifted to 334 nm with an increase in the glabridin concentration. Because β-lg has two tryptophan and four tyrosine residues in its monomeric state that contribute to the fluorescence, this result indicated that the interaction of glabridin with β-lg made the environment of Trp and Tyr residues more hydrophilic.[30]

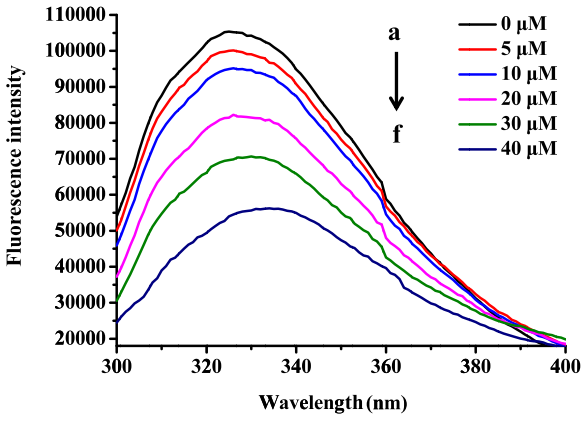

Figure 2. Fluorescence emission spectra of β-lg in the presence of glabridin at different concentrations at the excitation wavelengths of 280 nm in 10 mM phosphate buffer at pH 7.4 (a → f: 0, 5, 10, 20, 30, and 40 μM glabridin) at constant β-lg (10 μM).

The fluorescence spectra of the nanocomplexed glabridin with β-lg under different conditions is shown in Figure S1. As the pH of β-lg solution increased from 3.0 to 7.4, a decrease in fluorescence intensity was observed, while an increase at pH 10.0 (Figure S1a). This may be due to the transformation in the β-lg structure above pH 7 exposes more of the tyrosine and tryptophan residues.[31] Furthermore, the fluorescence intensity of the nanocomplexed glabridin with β-lg decreased with an increasing ionic strength (Figure S1b), whereas the fluorescence intensity increased with an increase in temperature (Figure S1c). These changes in protein fluorescent intensities may be related to the increasing structural stability the β-lg form a stable nanocomplex in high ionic strength[32] and changes in conformation of β-lg at elevated temperatures, affecting the binding efficiency of glabridin.

Water Solubility. According to the HPLC result (Figure S2 and Table S1, the Supporting Information), the calibration curve was linear over the range of 20−100 μg/mL with a correlation coefficient of $R^2 > 0.9998$. The solubility measurements showed that the solubility of the nanocomplexed glabridin with β-lg in deionized water was 0.231 ± 0.03 mg/mL, representing an increase of about 21 times compared to that of raw glabridin (0.011 ± 0.02 mg/mL). Thus, the solubility of glabridin was improved after complexing with β-lg. Aditya et al.[33] reported similar results in regards to the complexing of β-lg with curcumin. Hence, our results further contribute to a deeper understanding of β-lg as an attractive natural carrier for delivering important hydrophobic nutrients in aqueous systems.

Morphology and Crystal Form of Nanocomplexed Glabridin with β-lg. Scanning electron microscopy (SEM) was employed to visualize the surface morphology of glabridin, β-lg, the physical mixture, and the nanocomplexed glabridin with β-lg (Figure 3). Pure glabridin (Figure 3a) displayed prismatic crystals, whereas β-lg (Figure 3b) showed a blocky crystal morphology with many different sizes. Both individual crystal forms of glabridin and β-lg were observed in the SEM images of their physical mixture (Figure 3c). However, the nanocomplexed glabridin with β-lg (Figure 3d) appeared as structurally distinct not only from the free components but also from the physical mixture, confirming the formation of a new solid phase. This was similar with earlier result that has shown that β-lg had a marked effect on the morphology of micromolecule after the formation of the nanocomplex.[34]

Further evidence of the formation of the nanocomplexed glabridin with β-lg was provided by the XRD analysis. The XRD patterns of glabridin, β-lg, the physical mixture, and the nanocomplexed glabridin with β-lg are shown in Figure 4. Glabridin in its raw form (Figure 4a) exhibited strong and characteristic peaks at angles 8.5, 14.7, 16.2, 17.8, and 19.5, consistent with previous reports;[35] however, no distinct peaks were detected in the XRD patterns of β-lg (Figure 4b). Instead, the XRD patterns of β-lg showed a broad baseline signal not atypical for proteins.[36] In the diffraction peaks of the physical mixture, glabridin and β-lg showed identical peak pattern to

DOI: 10.1021/acsomega.8b01576
ACS Omega 2018, 3, 12246−12252

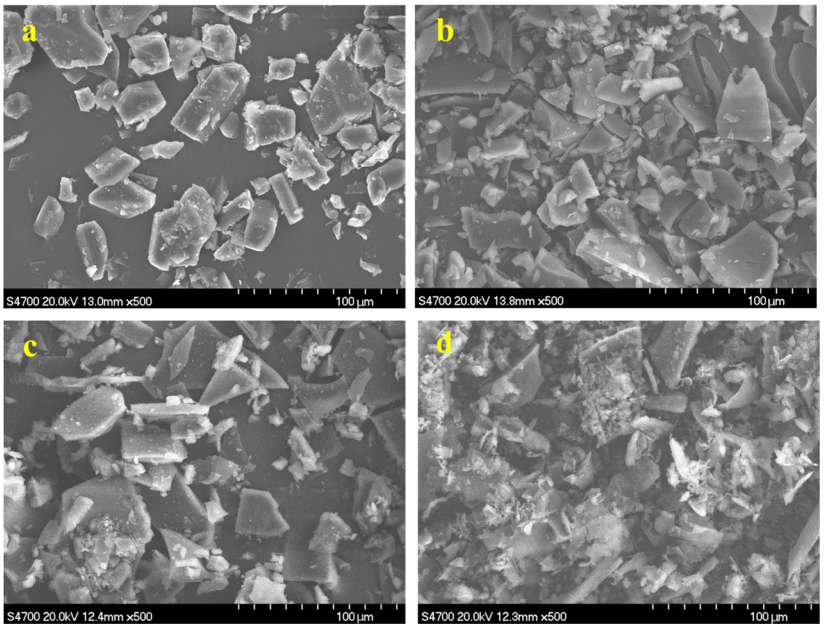

Figure 3. Scanning electron microscopy (SEM) of (a) glabridin, (b) β-lg, (c) the physical mixture, and (d) nanocomplexed glabridin with β-lg.

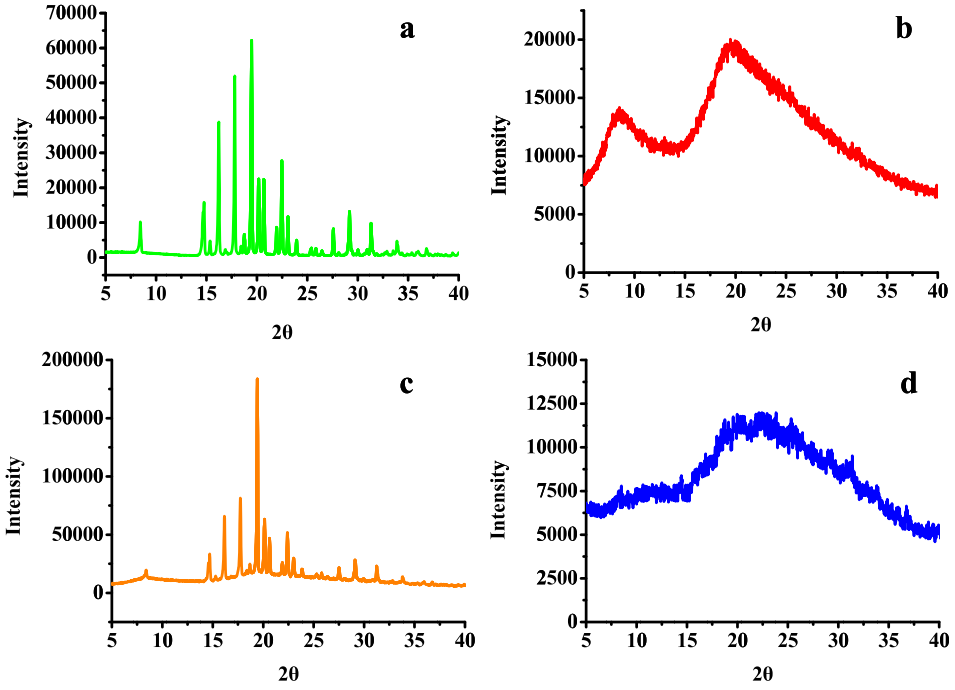

Figure 4. X-ray diffraction diagrams of (a) glabridin, (b) β-lg, (c) the physical mixture, and (d) the nanocomplexed glabridin with β-lg.

that of glabridin in its pure form, but at a lowered intensity (Figure 4c). This lowered intensity could be due to the fact that the presence of proteins (β-lg) partially hindered the transmission of the X-rays. Conversely, the nanocomplexed glabridin with β-lg showed no evidence of the XRD pattern associated with pure glabridin (Figure 4d). Instead, the signal was more typical of the XRD pattern of the β-lg XRD spectrum (Figure 4b) and that of proteins in their amorphous state,[37] which essentially translates in the total absence of any diffraction peaks corresponding to raw glabridin. This outcome may be the result of the complete nanocomplexing of free glabridin with β-lg, causing the absence of a typical set of diffraction peaks corresponding to glabridin.

Conformation of β-Lactoglobulin Loaded with Glabridin. FT-IR spectroscopy is a valuable method to monitor changes in the secondary structure of proteins and their dynamics when interacting with other compounds.[38,39] The FT-IR spectra of glabridin, β-lg, the physical mixture, and the nanocomplexed glabridin with β-lg are shown in Figure 5. Glabridin (Figure 5a) is characterized by distinct absorption peaks at 3340 cm^{-1} (for O−H stretching vibration), 1520 and 1480 cm^{-1} (for C═C stretching vibration in aromatic ring), 2970, 2920, and 1370 cm^{-1} (for CH_3 group), and 1270 cm^{-1} (for stretching of C−O−C). The peak position of the amide-I band of β-lg (Figure 5b) occurred at 1647 cm^{-1} (for C═O stretching, and representing an α-helix structure) and its

DOI: 10.1021/acsomega.8b01576
ACS Omega 2018, 3, 12246−12252

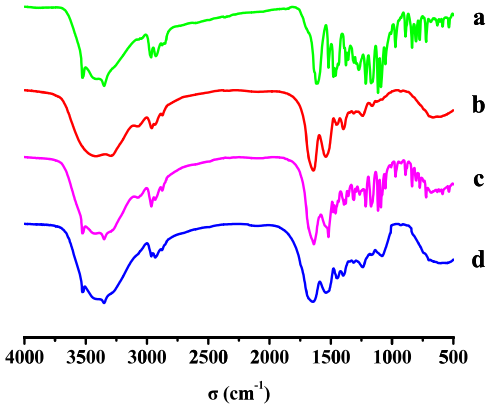

Figure 5. FT-IR spectra of (a) glabridin, (b) β-lg, (c) the physical mixture, and (d) the nanocomplexed glabridin with β-lg.

amide-II was displayed at 1539 cm^{-1} (C−N stretching coupled with N−H bending mode, and representing antiparallel β-sheet structures).[40] The FT-IR of the physical mixture (Figure 5c) was simply the superposition of the spectra of the individual component. The FT-IR spectrum of the nanocomplexed glabridin with β-lg (Figure 5d) showed a similar spectrum to the β-lg protein with the disappearance of glabridin, which was consistent with the XRD result. The peak position of β-lg shifted to 1639 cm^{-1} for amide-I and 1551 cm^{-1} for amide-II after interaction with glabridin signal. These results indicate a complex formation between β-lg and glabridin, following changes in the secondary structure and chemical microenvironments on the β-lg protein. Similar results were observed during the interaction between β-lg and the aliphatic compound bixin.[41]

To investigate the specific changes in the secondary structure of β-lg, both Omnic 8.0 and Peakfit 4.12 were employed to interpret the differences between the FT-IR data of pure β-lg protein and the nanocomplexed glabridin with β-lg in the range of 1600−1700 cm^{-1}. The content of α-helix almost did not change, with β-sheet and β-turn decreasing 3.8 and 2.8%, respectively (Table S2). And, the content of random coli increased 6.5%. This result confirmed that the conformation of β-lg changed after reacting with glabridin. The secondary structure of β-lg became loosen at the existence of glabridin's steric hindrance, which benefit to form hydrogen bonds between those two molecules and exposure the sleeping residues of protein.

Circular dichroism (CD) has been proven to be a useful technique to examine conformational changes that occur in the secondary structures of protein[42] as a result of changes in the microenvironmental conditions such as those caused by the binding/complexing of ligands.[43] Glabridin does not exhibit any CD bands in the aqueous solution (Figure S3). The CD spectrum of pure β-lg revealed a broad band with a minimum at 218 nm, which is characteristic of the presence of a prominent β-structure.[43] Following the nanocomplexing with glabridin, the band associated with the β-structure shifted to a higher wavelength of around 239 nm and the minimum became narrower and more negative. Furthermore, there were minor residual bands at 221 and 230 nm, which might be the evidence of the presence of noncomplexed β-lg. Changes in the CD spectra (Figure 6) suggest that the binding of β-lg with glabridin changed the secondary structures of β-lg,[44] which is consistent with the FT-IR result.

Molecular Docking Studies. To get further insight into and explain the experimental results obtained, a molecular modeling study was carried out using the AutoDock 4.2.6 software package to determine the potential mode of interaction between glabridin and β-lg. The proposed nanocomplexed glabridin with β-lg geometry showing the lowest energy is displayed in Figure 6. The inhibition constant and free energy of the binding of glabridin to β-lg were 883.92 nM and −8.26 kcal/mol, respectively. The molecular modeling also indicated that nine amino acid residues were involved in the docking of glabridin with β-lg. These included Ala139, Ala142, Met7, and Leu9, all of which possess hydrophobic residues and were very closely aligned with glabridin, meaning that there was substantial hydrophobic interaction between β-lg and glabridin. Furthermore, the three hydrogen bonds facilitated interactions between glabridin and β-lg. Specifically, 2′-OH and 4′-OH groups of the aromatic ring of the glabridin bonded with O atom of Ala139 and Thr4 of β-lg, respectively, where the OH group functioned as a hydrogen bond donor and the respective amino acid acted as the hydrogen bond acceptor; 1″-O of glabridin bonded with an amino group of Lys8 of β-lg, where the Lys was the hydrogen bond donor and O atom was the hydrogen bond acceptor. Based on our molecular modeling, it can be deduced that the interaction of glabridin with β-lg is not only via hydrophobic interactions but also through hydrogen bond formation.

In Vitro Bioactivity Assay. Natural compounds like flavonoids that possess potent antioxidant activity are strong scavengers of free radicals.[45] To evaluate the effectiveness of glabridin after nanocomplexing with β-lg as an antioxidant, the DPPH and ABTS radical-scavenging capacities were carried out. The DPPH radical-scavenging capacities of free glabridin and nanocomplexed glabridin with β-lg are shown in Figure 7a. The results indicate that increasing the concentration of

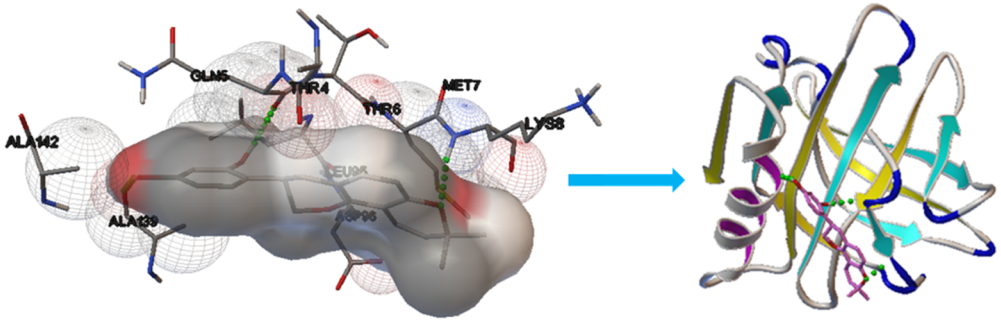

Figure 6. Best docked conformation and detailed view of the nanocomplexed glabridin with β-lg.

DOI: 10.1021/acsomega.8b01576
ACS Omega 2018, 3, 12246−12252

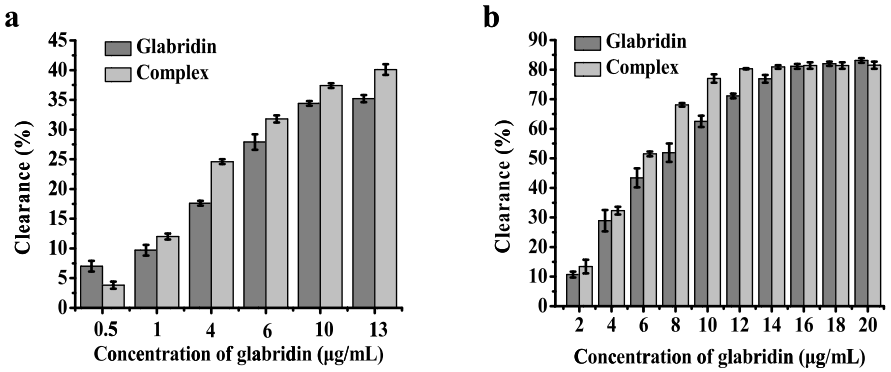

Figure 7. (a) DPPH radical-scavenging capacities and (b) ABTS radical-scavenging capacities of pure glabridin and the nanocomplexed glabridin with β-lg.

glabridin in the range of 0.5−13 μg/mL increases the scavenging capacities of both free and nanocomplexed glabridin. More specifically, the nanocomplexed glabridin asserted a greater radical-scavenging capacity compared to free glabridin alone. The ABTS radical-scavenging capacities of both free and nanocomplexed glabridin are shown in Figure 7b. The free radical clearance of free glabridin was 71.1%, whereas that of the nanocomplexed glabridin was 80.3% under the same concentration (12 μg/mL). Hence, both DPPH and ABTS radical-scavenging tests revealed that the nanocomplexed glabridin retained and even improved the free radical-scavenging capacity of glabridin (Figure 7a,b). The slight increase in the free radical-scavenging of the nanocomplexed glabridin maybe due to the notion that β-lg could control glabridin dosage, thus protecting glabridin against rapid oxidation by free radical and prolonging its antioxidant activity.

In conclusion, β-lg was used to as a carrier to encapsulate glabridin with a simple method of an antisolvent precipitation. In this study, changes in the β-lg fluorescence spectrum showed that the inclusion of glabridin made the microenvironment of the β-lg protein more hydrophobic. The results of SEM, XRD, FT-IR, CD, and molecular docking revealed that the nanocomplexed glabridin with β-lg was in amorphous form and the conformation of β-lg was changed after complexing with β-lg. Both hydrophobic interactions and hydrogen bonding contributed to the successful interaction between β-lg and glabridin. Based on the data obtained from in vitro bioactivity assay, nanocomplexed glabridin with β-lg retained its DPPH radical-scavenging capacity and its ABTS radical-scavenging capacity. Thus, β-lg can be considered as a good carrier and the nanocomplexed glabridin with β-lg could be a useful model of the drug−protein interaction. It would contribute to a deeper understanding of the molecular recognition properties of this lipocalin.

■ ASSOCIATED CONTENT

Supporting Information

The Supporting Information is available free of charge on the ACS Publications website at DOI: 10.1021/acsomega.8b01576.

Fluorescence spectra of β-lg with glabridin nanocomplexed with β-lg under different conditions, at an excitation wavelength of 280 nm: (a) fluorescence intensity influenced by pH, (b) fluorescence intensity influenced by variations in ionic strength, and (c) fluorescence intensity influenced by temperature; standard curve of glabridin; circular dichroism measurements of glabridin, β-lg, and the nanocomplexed glabridin with β-lg; concentration and related peak area of glabridin standard solution; content of different secondary structures of β-lg before and after nanocomplexing with glabridin (PDF)

■ AUTHOR INFORMATION

Corresponding Author

*E-mail: lianghao@mail.buct.edu.cn. Fax: +86 10 6443 7610.

ORCID

Hao Liang: 0000-0002-4799-882X

Notes

The authors declare no competing financial interest.

■ ACKNOWLEDGMENTS

The authors acknowledged financial support from the National Natural Science Foundation of China (21878014), the Beijing Natural Science Foundation (2162030), the Beijing Natural Science Foundation-Beijing Municipal Education Commission Joint Funding project (KZ201710020014), the Double First-rate Program (ylkxj03) and the 111 Project (B13005).

■ ABBREVIATIONS

β-lg, β-lactoglobulin
DPPH, 2,2-diphenyl-1-picrylhydrazyl radical
ABTS, 2,2′-azino-bis-3-ethylbenzthiazoline-6-sulfonic acid
SEM, scanning electron microscopy
XRD, X-ray diffractometry
FT-IR, Fourier transform infrared spectroscopy
CD, Circular Dichroism

■ REFERENCES

(1) Aoki, F.; Nakagawa, K.; Tanaka, A.; Matsuzaki, K.; Arai, N.; Mae, T. Determination of glabridin in human plasma by solid-phase extraction and LC-MS/MS. *J. Chromatogr. B: Anal. Technol. Biomed. Life Sci.* **2005**, *828*, 70−74.

(2) Belinky, P. A.; Aviram, M.; Fuhrman, B.; Rosenblat, M.; Vaya, J. The antioxidative effects of the isoflavan glabridin on endogenous constituents of LDL during its oxidation. *Atherosclerosis* **1998**, *137*, 49−61.

(3) Fukai, T.; Satoh, K.; Nomura, T.; Sakagami, H. Preliminary evaluation of antinephritis and radical scavenging activities of glabridin from *Glycyrrhiza glabra*. *Fitoterapia* **2003**, *74*, 624−629.

(4) Yokota, T.; Nishio, H.; Kubota, Y.; Mizoguchi, M. The inhibitory effect of glabridin from licorice extracts on melanogenesis and inflammation. *Pigm. Cell Res.* **1998**, *11*, 355−361.

DOI: 10.1021/acsomega.8b01576
ACS Omega 2018, 3, 12246−12252

(5) Nerya, O.; Vaya, J.; Musa, R.; Izrael, S.; Ben-Arie, R.; Tamir, S. Glabrene and isoliquiritigenin as tyrosinase inhibitors from licorice roots. *J. Agric. Food Chem.* **2003**, *51*, 1201−1207.
(6) Yehuda, I.; Madar, Z.; Leikin-Frenkel, A.; Tamir, S. Glabridin, an isoflavan from licorice root, downregulates iNOS expression and activity under high-glucose stress and inflammation. *Mol. Nutr. Food Res.* **2015**, *59*, 1041−1052.
(7) Simons, R.; Gruppen, H.; Bovee, T. F. H.; Verbruggen, M. A.; Vincken, J.-P. Prenylated isoflavonoids from plants as selective estrogen receptor modulators (phytoSERMs). *Food Funct.* **2012**, *3*, 810−827.
(8) Tamir, S.; Eizenberg, M.; Somjen, D.; Stern, N.; Shelach, R.; Kaye, A.; Vaya, J. Estrogenic and Antiproliferative Properties of Glabridin from Licorice in Human Breast Cancer Cells. *Cancer Res.* **2000**, *60*, 5704−5709.
(9) Yu, X.-Q.; Changli, C.; Zhou, X.-W.; Li, C.-G.; Du, Y.-M.; Liang, J.; Zhou, S.-F. In vitro and in vivo neuroprotective effect and mechanisms of glabridin, a major active isoflavan from *Glycyrrhiza glabra* (licorice). *Life Sci.* **2008**, *82*, 68−78.
(10) Ao, M.; Shi, Y.; Cui, Y.; Guo, W.; Wang, J.; Yu, L. Factors influencing glabridin stability. *Nat. Prod. Commun.* **2010**, *5*, 1907−1912.
(11) Albani, J. R.; Vogelaer, J.; Bretesche, L.; Kmiecik, D. Tryptophan 19 residue is the origin of bovine β-lactoglobulin fluorescence. *J. Pharm. Biomed. Anal.* **2014**, *91*, 144−150.
(12) Flower, D. R. The lipocalin protein family: structure and function. *Biochem. J.* **1996**, *318*, 1−14.
(13) Kontopidis, G.; Holt, C.; Sawyer, L. Invited review: beta-lactoglobulin: binding properties, structure, and function. *J. Dairy Sci.* **2004**, *87*, 785−796.
(14) Hasni, I.; Bourassa, P.; Tajmir-Riahi, H. A. Binding of Cationic Lipids to Milk β-Lactoglobulin. *J. Phys. Chem. B* **2011**, *115*, 6683.
(15) Devillegas, M.; Oria, R.; Sala, F.; Calvo, M. Lipid-binding by beta-lactoglobulin of cow milk. *Milchwissenschaft* **1987**, *42*, 357−358.
(16) Loch, J.; Polit, A.; Górecki, A.; Bonarek, P.; Kurpiewska, K.; Dziedzicka-Wasylewska, M.; Lewiński, K. Two modes of fatty acid binding to bovine β-lactoglobulin-crystallographic and spectroscopic studies. *J. Mol. Recognit.* **2011**, *24*, 341.
(17) Liu, J.; Jiang, L.; Zhang, Y.; Du, Z.; Qiu, X.; Kong, L.; Zhang, H. Binding behaviors and structural characteristics of ternary complexes of β-lactoglobulin, curcumin, and fatty acids. *RSC Adv.* **2017**, *7*, 45960−45967.
(18) Spector, A. A.; Fletcher, J. E. Binding of long chain fatty acids to β-lactoglobulin. *Lipids* **1970**, *5*, 403−411.
(19) Liang, L.; Tajmir-Riahi, H.; Subirade, M. Interaction of β-Lactoglobulin with Resveratrol and its Biological Implications. *Biomacromolecules* **2008**, *9*, 50−56.
(20) Sahihi, M.; Ghayeb, Y. An investigation of molecular dynamics simulation and molecular docking: Interaction of citrus flavonoids and bovine β-lactoglobulin in focus. *Comput. Biol. Med.* **2014**, *51*, 44−50.
(21) Riihimäki-Lampén, L. H.; Vainio, M. J.; Vahermo, M.; Pohjala, L. L.; Heikura, J. M.; Valkonen, K. H.; Virtanen, V. T.; Yli-Kauhaluoma, J. T.; Vuorela, P. M. The binding of synthetic retinoids to lipocalin beta-lactoglobulins. *J. Med. Chem.* **2010**, *53*, 514.
(22) Mensi, A.; Choiset, Y.; Rabesona, H.; Haertlé, T.; Borel, P.; Chobert, J.-M. Interactions of β-Lactoglobulin Variants A and B with Vitamin A. Competitive Binding of Retinoids and Carotenoids. *J. Agric. Food Chem.* **2013**, *61*, 4114−4119.
(23) Liang, L.; Subirade, M. Study of the acid and thermal stability of β-lactoglobulin−ligand complexes using fluorescence quenching. *Food Chem.* **2012**, *132*, 2023−2029.
(24) Sahihi, M.; Ghayeb, Y.; Bordar, A. K. Interaction of β-Lactoglobulin with Resveratrol: Molecular Docking and Molecular Dynamics Simulation Studies. *Chem. Biochem. Eng. Q.* **2013**, *27*, 417−422.
(25) Yang, M.-C.; Guan, H.-H.; Liu, M.-Y.; Lin, Y.-H.; Yang, J.-M.; Chen, W.-L.; Chen, C.-J.; Mao, S. J. T. Crystal structure of a secondary vitamin D_3 binding site of milk β-lactoglobulin. *Proteins: Struct., Funct., Bioinf.* **2008**, *71*, 1197−1210.
(26) Weber, C.; Coester, C.; Kreuter, J.; Langer, K. Desolvation process and surface characterisation of protein nanoparticles. *Int. J. Pharm.* **2000**, *194*, 91−102.
(27) Shimada, K.; Fujikawa, K.; Yahara, K.; Nakamura, T. Antioxidative properties of xanthan on the autoxidation of soybean oil in cyclodextrin emulsion. *J. Agric. Food Chem.* **1992**, *40*, 945−948.
(28) Li, X.; Lin, J.; Gao, Y.; Han, W.; Chen, D. Antioxidant activity and mechanism of Rhizoma Cimicifugae. *Chem. Cent. J.* **2012**, *6*, 140.
(29) Chen, X.; Ma, J.-M.; Yong, K.-L.; Lv, J.-C.; Zhang, X.-B. Fluorescence study on the interaction of human serum albumin with loureirin B. *Spectroscopy* **2010**, *24*, 547−557.
(30) Andrade, S. M.; Costa, S. M. B. Spectroscopic Studies on the Interaction of a Water Soluble Porphyrin and Two Drug Carrier Proteins. *Biophys. J.* **2002**, *82*, 1607−1619.
(31) Renard, D.; Lefebvre, J.; Griffin, M. C.; Griffin, W. G. Effects of pH and salt environment on the association of beta-lactoglobulin revealed by intrinsic fluorescence studies. *Int. J. Biol. Macromol.* **1998**, *22*, 41−49.
(32) Arakawa, T. The stabilization of β-lactoglobulin by glycine and NaCl. *Biopolymers* **1989**, *28*, 1397−1401.
(33) Aditya, N. P.; Yang, H.; Kim, S.; Ko, S. Fabrication of amorphous curcumin nanosuspensions using β-lactoglobulin to enhance solubility, stability, and bioavailability. *Colloids Surf., B* **2015**, *127*, 114−121.
(34) Aditya, N. P.; Yang, H.; Kim, S.; Ko, S. Fabrication of amorphous curcumin nanosuspensions using β-lactoglobulin to enhance solubility, stability, and bioavailability. *Colloids Surf., B* **2015**, *127*, 114−121.
(35) Wei, Y.; Zhang, J.; Zhou, Y.; Bei, W.; Li, Y.; Yuan, Q.; Liang, H. Characterization of glabridin/hydroxypropyl-beta-cyclodextrin inclusion complex with robust solubility and enhanced bioactivity. *Carbohydr. Polym.* **2017**, *159*, 152−160.
(36) Pujara, N.; Jambhrunkar, S.; Wong, K. Y.; McGuckin, M.; Popat, A. Enhanced colloidal stability, solubility and rapid dissolution of resveratrol by nanocomplexation with soy protein isolate. *J. Colloid Interface Sci.* **2017**, *488*, 303−308.
(37) Feng, T.; Wang, K.; Liu, F.; Ye, R.; Zhu, X.; Zhuang, H.; Xu, Z. Structural characterization and bioavailability of ternary nanoparticles consisting of amylose, alpha-linoleic acid and beta-lactoglobulin complexed with naringin. *Int. J. Biol. Macromol.* **2017**, *99*, 365−374.
(38) Teng, Z.; Li, Y.; Wang, Q. Insight into Curcumin-Loaded β-Lactoglobulin Nanoparticles: Incorporation, Particle Disintegration, and Releasing Profiles. *J. Agric. Food Chem.* **2014**, *62*, 8837−8847.
(39) Yue, Y.; Liu, J.; Liu, R.; Dong, Q.; Fan, J. Binding of helicid to human serum albumin: A hybrid spectroscopic approach and conformational study. *Spectrochim. Acta, Part A* **2014**, *124*, 46−51.
(40) Fang, Y.; Dalgleish, D. G. Conformation of β-Lactoglobulin Studied by FTIR: Effect of pH, Temperature, and Adsorption to the Oil−Water Interface. *J. Colloid Interface Sci.* **1997**, *196*, 292−298.
(41) Zhang, Y.; Wright, E.; Zhong, Q. Effects of pH on the Molecular Binding between β-Lactoglobulin and Bixin. *J. Agric. Food Chem.* **2013**, *61*, 947−954.
(42) Keiderling, T. A.; Lakhani, A. Mini review: Instrumentation for vibrational circular dichroism spectroscopy, still a role for dispersive instruments. *Chirality* **2018**, *30*, 238−253.
(43) Sneharani, A. H.; Karakkat, J. V.; Singh, S. A.; Rao, A. G. Interaction of curcumin with beta-lactoglobulin-stability, spectroscopic analysis, and molecular modeling of the complex. *J. Agric. Food Chem.* **2010**, *58*, 11130−11139.
(44) Sneharani, A. H.; Singh, S. A.; Rao, A. G. A. Interaction of α_{S1}-Casein with Curcumin and Its Biological Implications. *J. Agric. Food Chem.* **2009**, *57*, 10386−10391.
(45) Yu, J.; Wang, L.; Walzem, R. L.; Miller, E. G.; Pike, L. M.; Patil, B. S. Antioxidant activity of citrus limonoids, flavonoids, and coumarins. *J. Agric. Food Chem.* **2005**, *53*, 2009−2014.

DOI: 10.1021/acsomega.8b01576
ACS Omega 2018, 3, 12246−12252